

Mechanocatalysis for biomass-derived chemicals and fuels

Sandra M. Hick, Carolin Griebel, David T. Restrepo, Joshua H. Truitt, Eric J. Buker, Caroline Bylda and Richard G. Blair*

Received 4th November 2009, Accepted 8th December 2009

First published as an Advance Article on the web 25th January 2010

DOI: 10.1039/b923079c

Heterogeneous catalysis cannot be easily applied to solids such as cellulose. However, by mechanically grinding the correct catalyst and reactant, it is possible to induce solid–solid catalysis or mechanocatalysis. This process allows a wide range of solids to be effectively utilized as feedstock for commercially relevant compounds. Here we show a set of structural and physical parameters important for the implementation of catalysts in mechanocatalytic processes and their application in the catalytic depolymerization of cellulose. Using the best catalysts, which possess high surface acidities and layered structures, up to 84% of the available cellulose can be converted to water-soluble compounds in a single pass. This approach offers significant advantages over current methods - less waste, insensitivity to feedstock, multiple product pathways, and scalability. It can be easily integrated into existing biorefineries - converting them into multi-feedstock and multi-product facilities. This will expand the use of non-food polysaccharide sources such as switch grass.

1. Introduction

Lignocellulosic biomass represents a rich source of feedstock for fuels¹ and chemicals; major work in developing this resource is underway. Biological sources such as switch grass, corn stover, bagasse, and other agricultural waste are largely underutilized. Most lignocellulosic biomass is processed in one of three ways: acid hydrolysis, enzymatic hydrolysis, and pyrolysis.^{2,3} New biological^{4,5} and chemical⁶ approaches seek to circumvent the drawbacks associated with these processes.

Catalytic processing of these materials is an important topic. Although efficient catalysts have been developed for a wide range of heterogeneous systems, they are not suitable for solid–solid catalysis. A major difficulty with these solids is mass transport. High surface area structures suited to liquid and gas systems do not work as efficiently in solid systems. Two typical structures, porous solids and supported particles have limitations when applied to solid systems. Porous solids have pore sizes too small to accommodate molecules much larger than 30 Å; and supported particle systems still require some method to overcome the solid–solid diffusion barrier.

Biochemical pathways are also important in processing these polymers. However, enzymes have limited pressure/temperature regimes in which they can function and are not as robust as inorganic solids.

There are two issues that need to be addressed in order to realize effective catalysis in solid–solid reactions. The solid–solid diffusion barrier (mass transport) must be overcome and the catalyst must be structured to allow access to catalytic sites. Currently, most catalytic depolymerization involves solvent systems to overcome this diffusion barrier.^{7–10}

We have found that it is possible to overcome diffusion in a solid–solid reaction by using mechanical force without the addition of solvents. This phenomenon is often referred to as mechanocatalysis or tribocatalysis. Little work has been done on this phenomenon.^{11–14} In fact, recent work has focused on using traditional heterogeneous catalysts (such as zeolites) in mechanochemical processes.^{15–21} This approach ignores the aggressive nature of mechanical processing. Effective mechanocatalysts must be mechanically robust, and possess sites that are physically accessible and chemically active.

Mechanocatalytic processes require no external heat. All of the energy for the reaction comes from the pressures and frictional heating provided by the kinetic energy of milling media moving in a container. Although there is a large body of work examining mechanochemical syntheses,^{22–39} to date no one has examined the properties required for an effective mechanocatalyst.

In a mechanocatalytic system, it is important that intimate contact between the catalyst and reactant be maintained. Although most biomass processing facilities utilize some form of attrition technology, it is usually in the form of hammer mills, disk mills, or roller mills. These technologies are being actively researched,^{40–42} but they do not allow good interaction between a solid catalyst and the material being treated. Pebble (or rolling) mills, shaker mills, attrition mills, and planetary mills are a few examples of mills that effectively “push” the catalyst into contact with the material being treated (biomass).⁴³

Experimental

Reagents

Pure microcrystalline cellulose (Avicel, Brinkmann) was utilized to investigate the performance of different solid catalysts. The natural cellulose sources *Z. mays indurata* (flint corn),

University of Central Florida, Department of Chemistry, P.O. BOX 162366, Orlando, FL, 32816, USA, rblair@mail.ucf.edu; Fax: +1 407-823-2252; Tel: +1 407-823-0639

Prunus stone, paper, aspen wood, and mixed biomass were collected from local sources. The grasses: *A. gerardii* (Big Bluestem), *S. scoparium* (Little Bluestem) and *P. virgatum* (Switchgrass) were supplied by Agricol Corporation (Madison, WI). All natural cellulose sources were dried at room temperature to a moisture content of <10% and cut to 2 cm or smaller pieces.

The materials kaolinite (Edgar Plastic Kaolin, Axner Pottery), delaminated kaolinite (Kaopaque 10, IMERYS), aluminium phosphate (Fisher Scientific), aluminium oxide (J.T. Baker), talc (Nytol 100HR, Axner Pottery), Y-type zeolite (HS-320, Hydrogen Y, Wako Chemicals), bentonite (Asbury Carbons), vermiculite, quartz, muscovite mica, silicon carbide (-325 mesh, Electronic Space Products International), graphite (grade TC306, Asbury Carbons), and aluminium sulfate (Fisher Scientific) were used as received. Layered silicates were H⁺ exchanged by soaking in 1 M hydrochloric acid for 12 h, filtering and dried at 80 °C overnight. Chemically delaminated kaolinite was prepared by intercalating with urea and deintercalating by washing with water.⁴⁴ The super acid was prepared by stirring aluminium oxide (J.T. Baker) in 2.5 M H₂SO₄ followed by calcination at 600 °C.⁴⁵

Mechanical processing

Various amounts of cellulose and catalyst were ground using a rolling mill (custom), mixer mill (SPEX Certiprep, Metuchen, NJ), or attrition mill (Union Process Inc., Akron OH). Initial catalyst assessment was performed using a mixer mill. Typically, 2 grams of a 1 : 1 mixture of catalyst and cellulose were ground in a 65 mL vial (1.5" ID × 2.25" deep) made of 440C steel, utilizing three 0.5" balls made of the same material as the milling vial. Attrition milling experiments were performed by Union Process, Inc. in a 1-SD attrition mill run at 350 rpm with a 1.5 gallon tank, 40 lbs of 0.25" chrome steel (SAE 52100) balls as the milling media, and 1200 g of a 1 : 1 mixture of cellulose and catalyst. Rolling mill experiments were performed in a custom rolling mill constructed of 316 stainless steel with a diameter of 1.37" and a length of 4.93". The mill was charged with 25 0.5" balls made of 440C steel and 2 g of a 1 : 1 mixture of cellulose and catalyst.

Gravimetric analysis

The extent of hydrolysis was monitored gravimetrically. Conversion of cellulose to water-soluble oligosaccharides was determined by stirring 0.1 g of the reaction mixture in 30 mL of water. Any oligosaccharide with a degree of polymerization <5 will be solvated.⁴⁶ The production of water-soluble products was measured by filtration through a 47 mm diameter Whatman Nuclepore® track etched polycarbonate membrane filter with a pore size of 0.220 μm. The residue was dried in a 60 °C oven for 12 h and then weighed.

Gas chromatography with mass sensitive detection

GC-MS analysis was performed on an Agilent 6850 GC with an Agilent 19091-433E HP-5MS column (5% phenyl methyl siloxane, 30 m × 250 μm × 0.25 μm nom.) coupled with a 5975C VL mass selective detector. Saccharide composition was

analyzed by silanizing⁴⁷ the product. Dehydration products were extracted with 60 °C chloroform and analyzed by GC-MS.

Thin layer chromatography

Thin layer chromatography was used to assess the composition of the hydrolysis product. Solutions were spotted onto cellulose plates and developed with a 20 : 7 : 10 mixture of n-butanol, acetic acid, and water. The plates were stained with a 3% urea and 1 M phosphoric acid in n-butanol saturated water solution.

Discrete element modeling

Discrete element models of the milling process were generated using EDEM (DEM Solutions Ltd.).

Degree of polymerization

The degree of polymerization of the insoluble cellulose residue was determined using viscometry according to the method outlined in ASTM D 4243.

Results

Three milling modes were investigated for the mechanocatalytic depolymerization of cellulose—shaking, rolling, and stirring. Fig. 1 illustrates solubilization achievable in a SPEX shaker mill. No appreciable solubilization was realized on samples of microcrystalline cellulose milled without a catalyst.

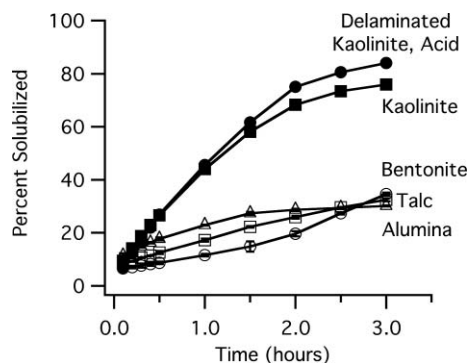


Fig. 1 Solubilization of cellulose as a function of milling time in a SPEX 8000D mixer mill. Catalysts were milled with microcrystalline cellulose in a 1 : 1 ratio. The most rapid solubilization was measured using 1 : 1 aluminosilicates such as kaolinite.

The catalysts' chemical and physical properties effect on conversion efficiency was studied by choosing materials with specific structural and chemical properties. Fig. 2 summarizes the solubilization results for cellulose mechanocatalytically treated for two hours in a shaker mill.

A shaker mill was chosen to assess catalyst efficacy since cellulose hydrolysis is observed after as little as 6 min of milling. This mode is a high-energy process with the possible realization of localized high pressures. After 3 h of milling, up to 84% of the cellulose can be converted to water-soluble fractions allowing rapid assessment of catalysts parameters.

The layered silicate mineral kaolinite was determined to be a good mechanocatalyst and the composition of the solubilized fraction produced was analyzed utilizing thin layer

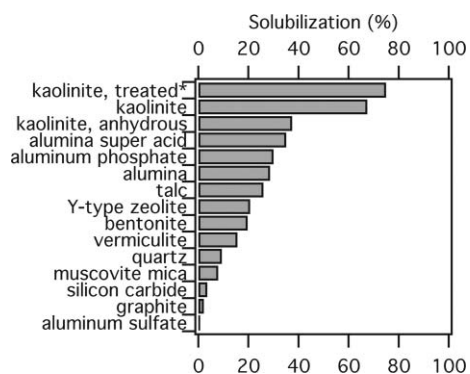


Fig. 2 Mechanocatalytic activity for a sample of compounds investigated. Catalysts were milled with microcrystalline cellulose in a 1 : 1 ratio for 2 h. Layered compounds with a surface acidity, H_0 , < -3.0 , as determined by dicinnamalacetone gave the best yields. The catalytic efficiency of kaolinite was improved through physical delamination and proton exchange (*).

chromatography and gas chromatography with mass sensitive detection. Both methods confirmed that depolymerization occurs rapidly with no oligosaccharides larger than $n = 2$ detected even after 30 min of treatment. The three major water-soluble components detected were levoglucosan, fructose, and glucose. The degree of polymerization of the insoluble residue was measured and found to decrease linearly with time.

The variation in product composition was studied as a function of milling mode and time. A study of the energy input through milling, and its effect on products, was investigated using a variable speed rolling-mill. Models were developed using discrete element methods (EDEMTM, DEM Solutions Ltd.) to estimate the compressive forces achieved during milling. These models indicate that, in a 10 s period, a shaker mill can produce 9 impacts with forces between 400 and 3000 N; an attrition mill can produce 9 impacts between 400 and 2000 N; a rolling mill at 30 rpm generates 4 impacts between 60 and 110 N; and at 100 rpm, 10 impacts between 60 and 130 N.

High-energy processing in a shaker mill resulted in the production of levoglucosan, fructose and glucose with a ratio of 9 : 1 : 4.3 after 30 min of treatment and a ratio of 4.6 : 1 : 4.1 after two hours of treatment. The product distribution was similar for samples prepared in an attrition mill. Low-speed processing in a rolling mill (30 rpm) resulted in no measurable catalytic activity; increasing the rotation velocity to 100 rpm resulted in $13.2 \pm 0.8\%$ solubilization after 96 h of treatment. The product consisted of levoglucosan, fructose, and glucose in a 1 : 1 : 5.8 ratio. With continued high energy milling the levoglucosan fraction decreased and other dehydration products were observed - levoglucosenone and 5-hydroxymethyl furfural (HMF), as well as the retro-aldol condensation product furfural (Fig. 3). This result is encouraging since HMF is of interest for use as a fuel or chemical feedstock.^{1,48,49}

Discussion

Milling alone (without a catalyst present) is not sufficient to hydrolyze the glycosidic bond in cellulose. Acidic solids such as kaolinite ($Al_2Si_2O_7 \cdot 2H_2O$), alumina super acid, aluminium phosphate ($AlPO_4$), alumina (Al_2O_3), Y-type zeolite,

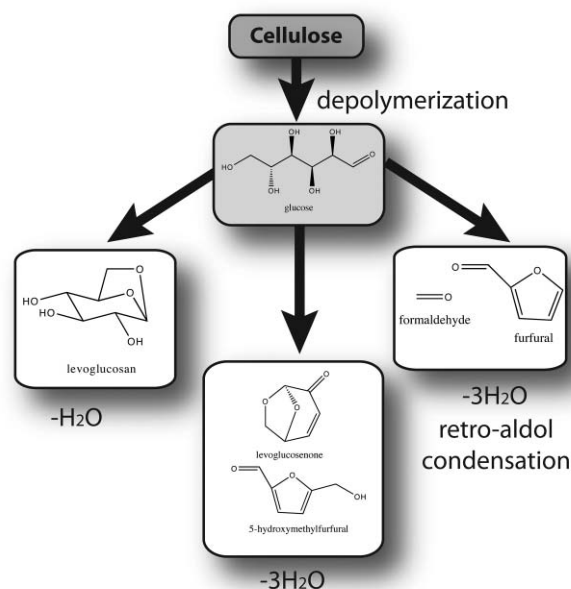


Fig. 3 Cellulose can be mechanocatalytically converted to glucose and, with prolonged treatment, into a variety of products. The formaldehyde produced was not observed with the analytical techniques utilized.

and bentonite ($Al_2Si_4O_{11} \cdot H_2O$) showed good catalytic ability. Low-acidity solids such as talc ($H_2Mg_3(SiO_3)_4$), vermiculite ($(MgFe,Al)_3(Al,Si)_4O_{10}(OH)_2 \cdot 4H_2O$), quartz (SiO_2), mica ($(KF)_2(Al_2O_3)_3(SiO_2)_6(H_2O)$), silicon carbide (SiC), graphite (C), and aluminium sulfate ($Al_2(SO_4)_3$) were less effective. The hardness of the catalyst did not play a role in the efficiency of the depolymerization. Both kaolinite and talc are soft, but kaolinite is a much more efficient catalyst. Silicon carbide and aluminium oxide are both very hard, but silicon carbide showed little or no catalytic ability. The use of harder catalysts resulted in undesirable wear on the container and milling media. The most effective catalyst is the layered mineral kaolinite. Kaolinite is an aluminosilicate consisting of aluminium-containing (as AlO_6 units) layers covalently bound to silicon-containing (as SiO_4 units) layers as in a 1 : 1 ratio. These layers are held together by hydrogen bonds from protons on open Al–O–Al sites to open Si–O–Si sites. The structurally similar bentonite has each aluminium-containing layer covalently bound above and below by a silicon-containing layer in a 2 : 1 configuration; this prevents the active sites from interacting with the cellulose (Fig. 4). The role of aluminium in the active sites was confirmed by comparing the catalytic ability of quartz and aluminium phosphate. These compounds are isostructural; substituting the SiO_4 units in quartz with AlO_4 and PO_4 units, as in aluminium phosphate, results in an increase in active sites and the observed increase in catalytic ability.

Layered compounds are effective mechanocatalysts because the layers are typically held together by weak forces such as hydrogen bonding and van der Waals forces. These bonds can be easily broken *via* mechanical processing (grinding or rubbing).⁵⁰ The result is a material with a high specific surface area (SSA) that is only dependent upon the number of layers in each particle.

$$SSA_{\text{hard sphere}} = \frac{3}{rd_{\text{solid}}} \quad (1)$$

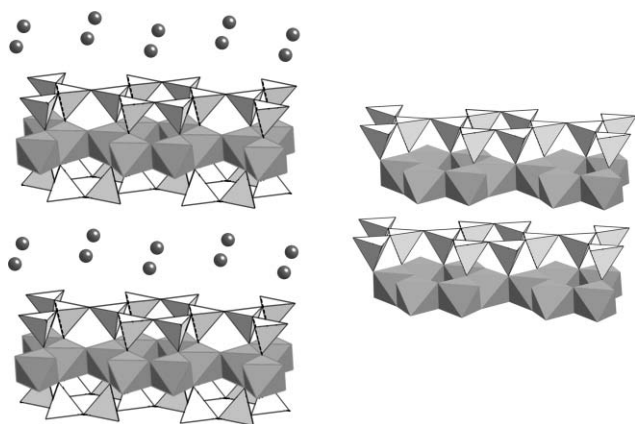


Fig. 4 The structures for the 2:1 smectite bentonite (left) and 1:1 smectite kaolinite (right). The octahedra are AlO_6 units and the tetrahedra are SiO_4 units. The sheets in bentonite are charged due to an Al:Si imbalance. The sheets are held together by ionic forces between the sheets and a cation (dark sphere). The sheets in kaolinite are held together by hydrogen bonds from protons on the Al layer to the oxygens on the Si layer.

$$SSA_{\text{layered}} = \frac{2}{(n + nf - 1)td_{\text{solid}}} \quad (2)$$

Eqn (1) and 2 give the specific surface areas (SSA) in area/unit mass for hard spheres and layered materials where n = the number of layers, d_{solid} = the density of the solid, r = the radius of the particle, t = the interlayer spacing, and f = the ratio of the layer thickness to the interlayer spacing. Eqn (1) is derived from the surface area of a solid sphere ($4\pi r^2$) and the mass of the sphere as determined by its density (mass = $4/3 \pi r^3 d_{\text{solid}}$). Eqn (2) is derived from the surface area of a fragment using its length and width ($2lw$) and the mass of n layers using the material's density and interlayer spacing (mass = $lw(n+nf-1)td_{\text{solid}}$). This derivation assumes both sides of the sheet are catalytically active. For kaolinite, only one side of the sheet (the AlO_6 side) is catalytically active. This results in a SSA half of that predicted by eqn (2). Using the $d_{\text{solid}} = 2.599 \text{ g cm}^{-3}$, $t = 2.892 \text{ \AA}$, and $f = 1.561$ for kaolinite, we find that reducing it to a collection of single aluminosilicate sheets (through delamination) would result in an active specific surface area of $852 \text{ m}^2 \text{ g}^{-1}$. This would be equivalent to 1.35 nm spherical particles. Structures consisting of 5 layers would have a specific surface area equivalent to 10.2 nm particles ($113 \text{ m}^2 \text{ g}^{-1}$). It has been suggested that mechanochemical processes are dependent on the area of surface sites available.¹⁵ This is in line with our observation that layered materials are the ideal structure for mechanocatalysts. Delamination of kaolinite to single sheets has been observed during grinding.⁵¹ In fact, it is not unreasonable to expect delamination to single layers; this has been observed in talc.¹⁵

It is important to note that anhydrous kaolinite showed a decrease in catalytic ability. This is due to the fact that water is required to break the cellulose glycosidic bond.

Kinetics and depolymerization mechanism

Concentrations in chemical reaction are typically expressed in terms of moles/l. In a solventless, solid-solid reaction this

expression is meaningless. If percent composition is used, the resulting expression does not accurately reflect the consequences of increasing the milling load without increasing the vessel size (which results in a decrease in reaction rate). We have found that reaction rates can be examined by expressing the concentration of reactants and products in terms of mass/free volume.⁵² Here the free volume is the volume of the milling container not occupied by balls, reactants, or products. This value is calculated by converting the masses of the reactants, products, and milling media to volumes based on the materials' densities. This volume is subtracted from the container volume to give a free volume. This approach indirectly incorporates the motions available to the milling media. The milling media, for the same mode of milling, in systems with large free volumes will have a greater mean free path than in systems with small free volumes.

We determined the reaction order by generating kinetic plots. Although attrition is quite rapid in a SPEX mill, finely ground cellulose (Avicel) and catalysts were used to minimize the effect of initial particle size. The reaction cannot be zeroth order since reaction rate would be independent of concentration. The concentration of the reactants directly affects the free volume and, subsequently, the motion of the milling media. Higher concentrations result in less motion. In the most severe case the concentration would be so high that no media motion is allowed. A zeroth order model would predict yield in this case - an unphysical prediction. Fig. 5 compares a first and second order plot in this system. The differentiation between first and second order behavior is a little more subtle. Both kinetic plots can be fit to lines representing initial and final kinetics. Although the first order plot gives slightly better linear correlation coefficients, a second order model more accurately describes the data. For example, using H^+ exchanged, physically delaminated kaolin the linear correlation coefficient for the initial kinetics is -0.9986 for first order kinetics and 0.9974 for second order kinetics. In the final kinetic region this coefficient is -0.9969 for first order kinetics and 0.9952 for second order kinetics. The important feature is the data point near the intersection of the two regression lines (inset Fig. 5). It does not fall on the first order curve that would be generated by the sum of the two linear fits. It does fall on the curve generated by the two linear second order fits. This behavior was observed for all catalysts listed in Table 1 which summarizes the rates observed in several systems. The uncertainties reported are the standard deviations in the slope of the second-order plot calculated using linear regression. The uncertainty in the time change was determined by propagating these uncertainties through the equation describing the intersection of these lines. Second order behavior has also been observed in the hydrolysis of the glucose dimer cellobiose in super critical water.⁵³

It was confirmed that the process was catalytic by performing turnover studies using kaolinite and cellulose in a shaker mill. Two hours of milling time resulted in loss of catalytic efficiency over 5 turnovers. One hour of milling resulted in no loss in catalytic efficacy over 8 turnovers. Although extended milling can induce significant defects in the crystal structure of the catalysts, the active sites on these catalysts are surface protons and should be unaffected by the defect structure of the solid. Prolonged milling may, instead, result in the formation of insoluble polymerization products. In particular,

Table 1 Second-order rates observed in the catalytic depolymerization of cellulose in a SPEX shaker mill. The column labeled “time change” indicates when the rate changes

	Initial Rate (second order) L g ⁻¹ h ⁻¹	Second Rate (second order) L g ⁻¹ h ⁻¹	Time Change (hours)
Kaolinite, physically delaminated, H ⁺ exchanged	0.0522 ± 0.0022	0.1460 ± 0.0058	1.21 ± 0.14
Kaolinite, H ⁺ exchanged	0.0464 ± 0.0017	0.0836 ± 0.0054	1.08 ± 0.29
Kaolinite, chemically delaminated	0.0433 ± 0.0013	0.0902 ± 0.0035	1.13 ± 0.15
Kaolinite, physically delaminated	0.0330 ± 0.0013	0.0832 ± 0.0027	1.16 ± 0.11
Kaolinite	0.03240 ± 0.00085	0.0825 ± 0.0056	0.75 ± 0.17
Bentonite	0.0268 ± 0.0015	0.00639 ± 0.00018	1.86 ± 0.18
Aluminium oxide	0.01147 ± 0.00050	0.00230 ± 0.00016	1.383 ± 0.049
Talc	0.00943 ± 0.00014	0.00415 ± 0.00026	3.567 ± 0.029

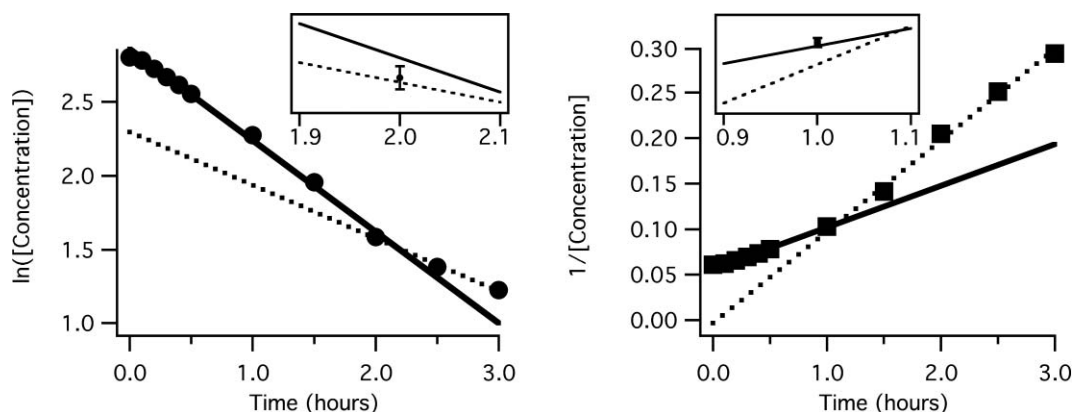


Fig. 5 A first (left) and second (right) order plot of the hydrolysis of cellulose in a SPEX shaker mill. Both plots show strong linear relations, but the data point near the intersection of the two fit lines (insets) indicates that a second-order process is the more accurate description. The catalyst used was H⁺ exchanged, physically delaminated kaolinite.

furfural polymerizes when heated in the presence of an acid. These insoluble by-products would interfere with the interaction between the catalyst and the reactant. Limiting the milling time limits the production of these by-products.

In order to understand the mechanism of cellulose depolymerization, the degree of polymerization (DP) of the insoluble residue was measured. This can be compared to the change in DP observed in acid and enzyme hydrolysis. The three approaches to depolymerization - acid, enzymatic, and mechanocatalytic proceed by quite different kinetics and mechanisms. By examining the change in degree of polymerization of the residue with respect to the fraction of oligomers with a DP < 5 (or degree of solubilization) the role of these factors can be reduced and the approaches can be compared.

Fig. 6 shows the change in DP as a function of degree of solubilization. Values for acid hydrolysis were simulated using a model that all bonds have an equal probability of cleavage.⁵⁴ Change in DP from enzyme hydrolysis was taken from the literature.⁵⁵ It can be seen that mechanocatalytic depolymerization does not follow a mechanism like acid or enzyme hydrolysis. Mechanocatalytic hydrolysis does not randomly cleave cellulose chains like acid hydrolysis. Initially, depolymerization more closely matches the enzymatic process. The accessibility of surface sites gives rise to the evolution of the degree of polymerization in enzyme hydrolysis.⁵⁶ Similarly, mechanocatalysis is dominated by two processes - attrition and hydrolysis. During the initial milling time, cellulose particles are being broken down physically and chemically. There are three main chemical reactions occurring. The reactions are: hydrolysis

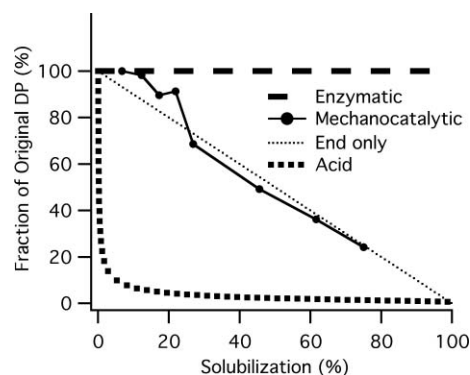


Fig. 6 Change in the degree of polymerization for the insoluble residue of cellulose hydrolysis as a function of degree of solubilization. The dotted line represents a model where hydrolysis only occurs at the ends of the polymer chain.

catalyzed by the catalyst’s surface protons, dehydration by the catalyst, and retro-aldol condensation due to the localized high pressures. The surfaces of these particles are accessible to the catalyst. At a certain point, attrition slows and only the end units of the cellulose chain are accessible. This results in a change in DP that coincides with a model where only the ends of a polymer chain are allowed to react (dashed line in Fig. 6). For the layered catalysts, bentonite, talc, and kaolinites the rate changes (Table 1) when solubilization is between 30 and 40%. This corresponds to the region in Fig. 6 where the DP of the residue matches an end-only hydrolysis model and further corroborates the second-order model.

Industrial applicability and economics

In order for mechanocatalysis to be an effective industrial tool, it must be effective for real world materials. We tested the conversion efficiency for a wide range of relevant cellulose sources. Fig. 7 illustrates the efficiency observed in the depolymerization of cellulose after two hours of milling in a mixer mill. Initial particle size was kept to less than 2 cm. In all cases, the cellulose source and catalyst were reduced to fine powders in 5 to 10 min due to the vigorous nature of the attrition process. Agricultural wastes from corn (corn stover), wood (aspen), and fruit (*Prunus* stone) production were examined; all showed improved water solubility after mechanocatalytic treatment. Commercial and residential waste such as paper and mixed waste from clearing land can also be efficiently treated. The grasses *A. gerardii* (Big Bluestem), *S. scoparium* (Little Bluestem) and *P. virgatum* (Switchgrass) are crops that are of interest for use as a biomass source. It should be noted that 90% of a corn kernel's mass can be converted to soluble matter in a single pass.

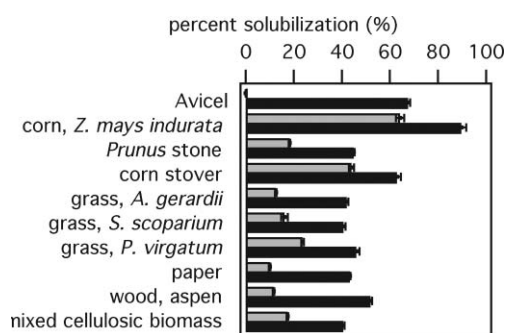


Fig. 7 Unlike current approaches to cellulose hydrolysis, mechanocatalytic hydrolysis is relatively insensitive to feedstock.

Our survey experiments have utilized a SPEX mixer mill, which allows us to rapidly assess the viability of catalytic materials and develop kinetic models for cellulose conversion. We have found that the reaction goes as a second-order process in cellulose. However, this technology is not scalable without significant redesign.⁵⁷ Rolling-mode and stirring-mode are among the scalable approaches. Utilizing our DEM model, it was determined that rolling mills do not develop the high pressures encountered in a shaking mill. Processing in a rolling mill produced a product composed primarily of glucose. This suggests that the forces that occur during the milling process are directly related to the composition of the soluble fraction produced. Low forces result in no observable solubilization; increasing the rotational velocity of the roller mill results in compressive forces and a measurable yield of sugars. The most energetic process, shaking-mode, results in an increase in the levoglucosan fraction. This implies that there is a critical energetic region favorable for the production of fructose and glucose.

Attritors are scalable, can be run in a batch or continuous mode, and can produce compressive forces similar to those achieved in a shaker mill (0.4 to 3 GPa, as predicted by our DEM models). We performed a limited number of kilogram-scale tests using a small Union Process attritor. Fig. 8 illustrates the energy costs associated with the two milling technologies. The dashed line is the energy obtainable from the ethanol produced from

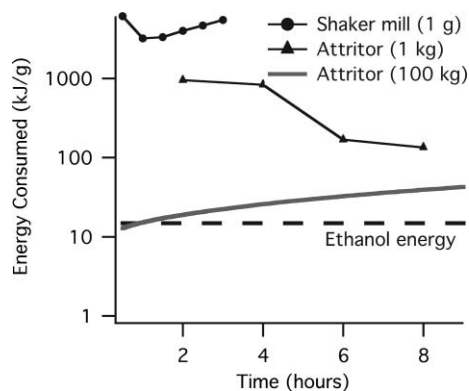


Fig. 8 The energy consumed to produce 1 gram of glucose from 1 gram of cellulose treated in a shaker mill, 1 kg of cellulose treated in an attritor, and modeled consumptions for 100 kg in a large attritor. The dashed line is the energy released by burning the ethanol produced from 1 gram of glucose.

one gram of glucose. It can be seen that the SPEX mill is an energy intensive process. Switching to an attritor allowed the process to be scaled-up by 1000 fold; the result was nearly a 46-fold decrease in the energy consumption as expressed in kJ/gram glucose produced. It was found that conversion in a small attritor required a 4-hour initiation time before the rate became appreciable. The kinetic data from this batch was used, in conjunction with the behavior observed in the shaker mill, to develop a predictive model for a 100 kg batch. The gray trace in Fig. 8 shows the projected energy consumption for an attritor with a 150 hp motor and fast reaction kinetics. It is important to note that the four-hour induction period must be eliminated for this approach to produce glucose at an energy cost lower than the energy released by burning the ethanol prepared from the glucose. This process is energy positive for 0.9 h of milling with a predicted conversion efficiency of 20.2%.

Conclusions

The natural layered structure of clays is ideally suited for use as a catalyst in milling processes. We have shown that layered structures are particularly suited to mechanocatalytic processes. This opens up a new area for catalyst synthesis. A new set of catalysts based on this paradigm could be synthesized to take advantage of the unique conditions in a ball mill. Using this idea, it may be possible to depolymerize other biopolymers such as chitin or protein as well as synthetic polymers such as nylon, polyethylene terephthalate, polycarbonate, and polylactic acid.

The observation of the glucose dehydration products levoglucosan, levoglucosenone, and 5-hydroxymethylfurfural as well as the retro-aldol condensation product furfural suggest that it will be possible to design mechanocatalysts for the direct conversion of cellulose into these compounds. In fact, many of the synthetic pathways utilized to produce derivatives from these compounds should be directly accessible through solventless milling.

Mechanocatalytic processing of materials has significant advantages over current methods. The best catalyst so far, kaolinite, costs around \$80/ton and can be reused. Any catalyst waste produced is innocuous and there are no toxic solvents needed. Additionally, no heating or high-pressure equipment is

required, simplifying plant design. Mechanocatalytic conversion of cellulose is insensitive to lignin and hemicellulose content allowing any cellulosic biomass source to be utilized. This is an improvement over methods that utilize edible biomass (such as corn) for ethanol production.

Dedication

This manuscript is dedicated to the memory of Glenn T. Blair (1945–2009).

Acknowledgements

We thank Agricol Corporation (Madison, WI) for supplying samples of Big Bluestem, Little Bluestem, and Switch grass; IMERYS (Roswell, GA) for supplying samples of physically delaminated kaolinite; and Asbury Carbons (Asbury, NJ) for supplying samples of bentonite and graphite.

References

- 1 G. W. Huber, S. Iborra and A. Corma, *Chem. Rev.*, 2006, **106**, 4044–4098.
- 2 S. J. B. Duff and W. D. Murray, *Bioresour. Technol.*, 1996, **55**, 1–33.
- 3 A. Demirbas and G. Arin, *Energy Sources*, 2002, **24**, 471–482.
- 4 M. B. Sticklen, *Nat. Rev. Genet.*, 2008, **9**, 433–443.
- 5 T. S. Bayer, D. M. Widmaier, K. Temme, E. A. Mirsky, D. V. Santi and C. A. Voigt, *J. Am. Chem. Soc.*, 2009, **131**, 6508–6515.
- 6 Y. Zhao, W.-J. Lu, H.-T. Wang and D. Li, *Environ. Sci. Technol.*, 2009, **43**, 1565–1570.
- 7 R. Rinaldi, R. Palkovits and F. Schuth, *Angew. Chem., Int. Ed.*, 2008, **47**, 8047–8050.
- 8 T. Iwaya, S. Tokuno, M. Sasaki, M. Goto and K. Shibata, *J. Mater. Sci.*, 2008, **43**, 2452–2456.
- 9 J. Shabtai, X. Xiao and W. Zmierzczak, *Energy Fuels*, 1997, **11**, 76–87.
- 10 R. W. Thring and J. Breau, *Fuel*, 1996, **75**, 795–800.
- 11 T. Ohta, *Appl. Energy*, 2000, **67**, 181–193.
- 12 A. Karpinska, C. Kajdas and K. i. Hiratsuka, *Tribologia*, 2006, **37**, 21–37.
- 13 C. Kajdas and A. Karpinska, *Tribologia*, 2005, **36**, 125–141.
- 14 Y. Momose, *Toraiborojisuto*, 2001, **46**, 391–397.
- 15 M. Hasegawa, M. Kimata and I. Takahashi, *Adv. Powder Technol.*, 2007, **18**, 541–554.
- 16 S. Ikeda, T. Takata, M. Komoda, M. Hara, J. N. Kondo, K. Domen, A. Tanaka, H. Hosono and H. Kawazoe, *Phys. Chem. Chem. Phys.*, 1999, **1**, 4485–4491.
- 17 S. Ikeda, T. Takata, T. Kondo, G. Hitoki, M. Hara, J. N. Kondo, K. Domen, H. Hosono, H. Kawazoe and A. Tanaka, *Chem. Commun.*, 1998, 2185–2186.
- 18 S. Murakami, M. Tabata and J. Sohma, *J. Appl. Polym. Sci.*, 1984, **29**, 291–298.
- 19 C. Kajdas, K. Hiratsuka and A. Borkowska, *Tribologia*, 2004, **35**, 11–25.
- 20 T. Shirasaki, *Shikizai Kyokaishi*, 1972, **45**, 737–743.
- 21 S. Murakami, M. Tabata, J. Sohma and M. Hatano, *J. Appl. Polym. Sci.*, 1984, **29**, 3445–3455.
- 22 E. Barraud, S. Begin-Colin, G. Le Caer, O. Barres and F. Villieras, *J. Alloys Compd.*, 2008, **456**, 224–233.
- 23 M. K. Beyer and H. Clausen-Schaumann, *Chem. Rev. (Washington, DC, U. S.)*, 2005, **105**, 2921–2948.
- 24 V. V. Boldyrev and K. Tkacova, *J. Mater. Synth. Process.*, 2000, **8**, 121–132.
- 25 P. G. Fox, *J. Mater. Sci.*, 1975, **10**, 340–369.
- 26 S. Granick and S. C. Bae, *Nature*, 2006, **440**, 160–161.
- 27 S. Kipp, V. Sepelak and K. Dieter Becker, *Chem. Unserer Zeit*, 2005, **39**, 384–392.
- 28 B. Kubias, M. J. G. Fait and R. Schloegl, *Handb. Heterog. Catal. (2nd Ed.)*, 2008, **1**, 571–583.
- 29 V. I. Levitas, *Phys. Rev. B: Condens. Matter Mater. Phys.*, 2004, **70**, 184118.
- 30 B. Rodríguez, A. Bruckmann, T. Rantanen and C. Bolm, *Adv. Synth. Catal.*, 2007, **349**, 2213–2233.
- 31 B. M. Rosen and V. Percec, *Nature*, 2007, **446**, 381–382.
- 32 L. Takacs, *Hyperfine Interact.*, 1997, **111**, 245–250.
- 33 Z. V. Todres, in *Organic Mechanochemistry and Its Practical Applications*, CRC Taylor and Francis, Boca Raton, FL, 2006, pp. 61–102.
- 34 F. K. Urakaev and V. V. Boldyrev, *Powder Technol.*, 2000, **107**, 93–107.
- 35 F. K. Urakaev and V. V. Boldyrev, *Powder Technol.*, 2000, **107**, 197–206.
- 36 K. Wieczorek-Ciurowa and K. Gamrat, *Mater. Sci.*, 2007, **25**, 219–232.
- 37 H. Yang and P. G. McCormick, *Trans. Mater. Res. Soc. Jpn.*, 1994, **14A**, 617–620.
- 38 I. J. Lin and S. Nativ, *Mater. Sci. Eng.*, 1979, **39**, 193–209.
- 39 G. Kaupp, *CrystEngComm*, 2009, **11**, 388–403.
- 40 L. S. Esteban and J. E. Carrasco, *Powder Technol.*, 2006, **166**, 139–151.
- 41 D. Schell and C. Harwood, *Appl. Biochem. Biotechnol.*, 1994, **45–46**, 159–168.
- 42 V. S. P. Bitra, A. R. Womac, N. Chevanan, P. I. Miu, C. Igathinathane, S. Sokhansanj and D. R. Smith, *Powder Technol.*, 2009, **193**, 32–45.
- 43 C. Suryanarayana, *Prog. Mater. Sci.*, 2001, **46**, 1–184.
- 44 K. Tsunematsu and H. Tateyama, *J. Am. Ceram. Soc.*, 1999, **82**, 1589–1591.
- 45 K. Arata, *Appl. Catal., A*, 1996, **146**, 3–32.
- 46 J. B. Taylor, *Trans. Faraday Soc.*, 1957, **53**, 1198–1203.
- 47 M. L. Sanz, J. Sanz and I. Martínez-Castro, *J. Chromatogr., A*, 2004, **1059**, 143–148.
- 48 J. N. Chheda, Y. Roman-Leshkov and J. A. Dumesic, *Green Chem.*, 2007, **9**, 342–350.
- 49 Y. Roman-Leshkov, J. N. Chheda and J. A. Dumesic, *Science*, 2006, **312**, 1933–1937.
- 50 J. Kano and F. Saito, *Powder Technol.*, 1998, **98**, 166–170.
- 51 S. Yariv and I. Lapidés, *J. Mater. Synth. Process.*, 2000, **8**, 223–233.
- 52 S. M. Hick, C. Griebel and R. G. Blair, *Inorg. Chem.*, 2009, **48**, 2333–2338.
- 53 M. Sasaki, M. Furukawa, K. Minami, T. Adschiri and K. Arai, *Ind. Eng. Chem. Res.*, 2002, **41**, 6642–6649.
- 54 R. Simha, *J. Appl. Phys.*, 1941, **12**, 569–578.
- 55 Y. H. P. Zhang and L. R. Lynd, *Biomacromolecules*, 2005, **6**, 1510–1515.
- 56 Y. H. P. Zhang and L. R. Lynd, *Biotechnol. Bioeng.*, 2004, **88**, 797–824.
- 57 G. Janke, A. Frenzel and G. Schmidt-Naake, *Chem. Eng. Technol.*, 1999, **22**, 997–1000.